DOI https: //doi. org/10.1007/s11595-018-1959-9

Isothermal Crystallization Kinetics of Nylon 10T and Nylon 10T/1010 Copolymers: Effect of Sebacic Acid as a Third Comonomer

WANG Zhongqiang[1,2], HU Guosheng[1*], ZHANG Jingting[1], XU Jiusheng[2], SHI Wenbo[1]

(1. Institute of Macromolecules and Bioengineering, School of Materials Science and Engineering, North University of China, Taiyuan 030051, China; 2. Guangdong Sinoplast Advanced Material Co. Ltd. , Dongguan 523860, China)

Abstract: Nylon 10T and nylon 10T/1010 samples were synthesized by direct melt polymerization. The isothermal crystallization kinetics of nylon 10T and nylon 10T/1010 was investigated by means of differential scanning calorimetry (DSC). The crystallization kinetics under isothermal condition has been analyzed by the Avrami equation. It was found that the Avrami equation was well-suited to describe the isothermal crystallization kinetics, combined with the results of the Turnbull-Fisher equation. The values of T_m^0 and K_g were obtained by Hoffman-Weeks and Lauritzen-Hoffman equations, respectively. The activation energies for isothermal crystallization of nylon 10T and nylon 10T/1010 were determined using the Arrhenius equation and found to be -123.24 and -81.86 kJ·mol^{-1}, respectively, which reveals that the crystallization ability of nylon 10T/1010 was lower than that of nylon 10T during the isothermal crystallization process. The crystal morphology was observed by means of polarized optical microscopy (POM) and X-ray diffraction (XRD). It was found that the addition of sebacic acid comonomer did not change the crystal form of nylon 10T, but significantly increased the number and decreased the size of spherulites.

Key words: melt polymerization; nylon 10T; nylon 10T/1010; semiaromatic polyamides; crystallization kinetics; isothermal crystallization

1 Introduction

Nylons, also known as polyamides, are a class of engineering thermoplastics used in a wide variety of applications[1,2]. They can be economically produced by melt processing, but their poor thermal properties, poor dimensional stability and high water absorption limit their applications in several industrial fields, especially in manufacture of the LED reflectors, the shells of automobile engines and in the surface mount technology (SMT)[3]. For improving the thermal properties of nylons, aromatic rings have been incorporated into their backbones to give more robust materials, such as poly(hexamethylene terephthalamide) (nylon 6T) copolymers[4,5], poly(nonamethylene terephthalamide) (nylon 9T)[6,7], poly(decamethylene terephthalamide) (nylon 10T)[8,9], and poly(dodecamethylene terephthalamide) (nylon 12T)[10,11]. In particular, nylon 10T, a condensation type polymer containing 1,10-decanediamine and terephthalic acid, is a good engineering plastic with good thermal durability and low water absorption. However, nylon 10T has a high melting point, as high as 315 °C[12], which is close to its decomposition temperature. Hence, the melt processing window is narrow, which limits its scope in industrial processing and applications. Sebacic acid can be used as a comonomer to reduce the melting temperature of nylon 10T by reducing the contents of aromatic rings structure, while still maintaining the excellent mechanical properties of the poly(decamethylene terephthalamide/decamethylene decanediamide) (nylon 10T/1010) copolymer. Furthermore, 1,10-decanediamine and sebacic acid are both important starting materials used to synthesize nylon 10T/1010 and can be obtained from the product of castor oil, which in turn is obtained from processing of castor seeds[13]. Therefore, nylon 10T/1010 can be considered a type of green material which is obtained

(Received: May 15, 2016; Accepted: July 25, 2018)

WANG Zhongqiang(王忠强): Ph D; E-mail: jaw1985@sina.com

*Corresponding author: HU Guosheng(胡国胜): Prof.; E-mail: huguosheng@nuc.edu.cn

Supported by the National Science and Technology Support Program of China (No. 2013BAE02B01), the Special Project on the Integration of Industry, Education and Research of Guangdong Province (No. 2013B090500003), and the Commissioner Workstation Project of Guangdong Province (No. 2014A090906002)

from natural raw materials[14].

It is well known that the mechanical and thermal properties of semi-crystalline polymers, such as nylons, strongly depend on their crystalline structures, degree of crystallization and morphologies, all of which are significantly controlled by the crystallization stage during the polymer molding process[15]. Polymer molding technologies including extrusion molding, injection molding and film-forming are often performed under isothermal or non-isothermal conditions in practical applications[16]. In addition, isothermal crystallization is very amenable to theoretical analysis[17-20]. Although some studies have synthesized a series of semiaromatic polyamides, few studies have focused on the crystallization kinetics of nylon 10T and nylon 10T/1010[2,3,8,9]. For this reason, we have performed an isothermal crystallization kinetics study based on differential scanning calorimetric measurements.

In this work, Avrami, Hoffman-Weeks, Turnbull-Fisher and Lauritzen-Hoffman equations were applied to discuss the isothermal crystallization kinetics of the nylon 10T and nylon 10T/1010 copolymers. Moreover, the activation energy for isothermal crystallization was calculated using the Arrhenius equation. Finally, the crystal morphologies of the two polymers were studied by polarized optical microscopy (POM) and X-ray diffraction (XRD).

2 Experimental

2.1 Materials

Terephthalic acid and benzoic acid were purchased from Beijing Yanshan Lithification Chemical Co. Ltd. (Beijing, China). 1,10-Decanediamine and sebacic acid were supplied by Wuxi Xinda Nylons Co. Ltd. (Wuxi, China).

2.2 Synthesis

Nylon 10T/1010 was synthesized via a direct melt polymerization process which included three steps, namely, prepolymerization, final polycondensation and viscosity increasing reaction, as shown in Fig.1.

In a typical procedure, 1,10-decanediamine (172.3 g, 1 mol), terephthalic acid (149.5 g, 0.9 mol), sebacic acid (20.2 g, 0.1 mol) and benzoic acid (6.1 g, 0.05 mol) were added into a polymerization kettle and distilled water (150 g) was added to reduce the volatilization of diamine during the polymerization. Benzoic acid was used as the inhibitor in order to control the molecular weight of nylon 10T/1010. The polymerization kettle was filled with nitrogen at room temperature and then heated to 275 ℃ in 3 h, meanwhile the pressure was up to 2.0 MPa. After 1.5 h, the pressure of the polymerization kettle was gradually decreased to atmospheric pressure in 1 h by deflating and the reaction temperature of the polymerization kettle was increased to 310 ℃. After reaction for another 0.5 h, the pressure of the polymerization kettle was evacuated to -0.099 MPa and the viscosity increasing reaction was allowed to proceed for 0.3 h. Finally, the polymerization kettle was cooled to room temperature and nylon 10T/1010 was obtained (327 g, 94%).

Nylon 10T was prepared by the similar procedure, except that sebacic acid was not added. In a typical reaction, only 1,10-decanediamine (172.3 g, 1 mol), terephthalic acid (166.1 g, 1 mol) and benzoic acid (6.1 g, 0.05 mol) were used, and nylon 10T was obtained (320 g, 93%). The intrinsic viscosity values ([η]) of nylon 10T and nylon 10T/1010 were 83 and 87 mL·g^{-1}, respectively.

2.3 Characterization

2.3.1 Intrinsic viscosity

The intrinsic viscosities of the nylon 10T and nylon 10T/1010 copolymers were determined in concentrated sulfuric acid with an Ubbelohde viscometer at (25 ± 0.1)℃.

2.3.2 FT-IR

FT-IR spectra were recorded on a Shimadzu 8400S spectrometer (Japan). The samples were prepared by melt-pressing as KBr discs.

2.3.3 Differential scanning calorimetry

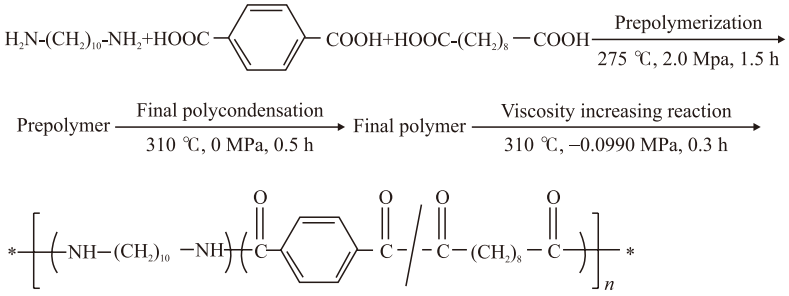

Fig.1 Schematic representation of the polymerization processes of nylon 10T/1010

The isothermal crystallization was carried out by using a Mettler Toledo 822e differential scanning calorimeter (Switzerland). All DSC measurements were performed in a nitrogen atmosphere. The weight of the samples was approximately 3 mg. The thermal history of the samples was eliminated by heating the samples at 330 ℃ for a period of 5 min. In the isothermal crystallization process, the samples were quenched at 100 ℃·min^{-1} from 330 ℃ to the desired crystallization temperature (T_c) and kept there for a period of time until complete crystallization.

2.3.4 Polarized optical microscopy

Polarized optical microscopic (POM) images were obtained by using a XPT-7 microscope (Optical Instruments Factory, Shanghai, China). Nylon 10T and nylon 10T/1010 samples were observed in thin films prepared between microscope coverslips by melting the polymer at 315 ℃ for 2 min and then rapidly cooling to the crystallization temperature in an automatic hot stage. The nylon 10T and the nylon 10T/1010 samples were isothermally crystallized for 0.5 h at the temperatures of 269 and 260 ℃, respectively. The images were recorded after complete crystallization.

2.3.5 X-ray diffraction

The crystal structures of nylon 10T and nylon 10T/1010 were examined by a D/max-RB X-ray diffractometer (Rigaku Industrial Corporation, Japan) using X-ray tube (40 kV, at 100 mA) and Cu Kα radiation at ambient temperature. The scanning rate was set as 5 °·min^{-1} in the range from 5° to 50°. The XRD data were analyzed by using MDI Jade 5.0 software from American Materials Data Corporation.

3 Results and Discussion

3.1 Fourier transform infrared spectra

FT-IR spectra of the nylon 10T/1010 salt and the nylon 10T/1010 are shown in Fig.2. The characteristic peaks of the nylon 10T/1010 salt were observed at 3 392 cm^{-1} (NH_3^+, N-H stretching vibration) and 2 143 cm^{-1} (NH_3^+, the absorption peaks of frequency doubling and combination band) . The characteristic peaks of amide groups of the nylon 10T/1010 were found at 3 129 cm^{-1} (hydrogen-bonded and N-H stretching vibration), 1 643 cm^{-1} (C=O stretching vibration), and 1 400 cm^{-1} (C-N stretching and CO-N-H bending vibrations), respectively. Comparing the FT-IR spectra of nylon 10T/1010 salt and nylon 10T/1010, it can be seen that one of the characteristic absorption peaks of the nylon 10T/1010 around 2 143 cm^{-1} (NH_3^+) has disappeared. The results indicate that nylon 10T/1010 can be synthesized via direct melt polymerization, as per the process depicted in Fig.1.

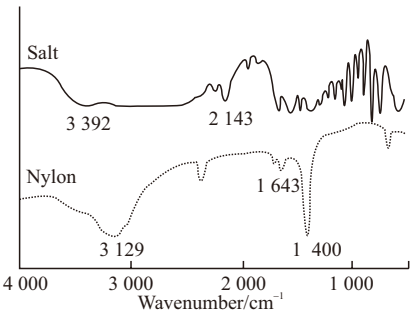

Fig.2 FT-IR spectra of nylon 10T/1010 salt and nylon 10T/1010

3.2 Isothermal crystallization behaviors

The isothermal crystallization thermograms of nylon 10T and nylon 10T/1010 samples were obtained by cooling the polymer melt to the specified crystallization temperature, and are shown in Fig.3. It can be seen that the crystallization peaks of nylon 10T and nylon 10T/1010 shifted to the right and became flatter with increasing crystallization temperature. This indicates that the crystallization rate decreased with an increase in the crystallization temperature and the samples required longer time to achieve complete crystallization at higher crystallization temperatures. In the case of nylon 10T/1010, the crystallization peaks shifted to lower isothermal crystallization temperatures due to the addition of the sebacic acid comonomer.

In order to better understand the isothermal

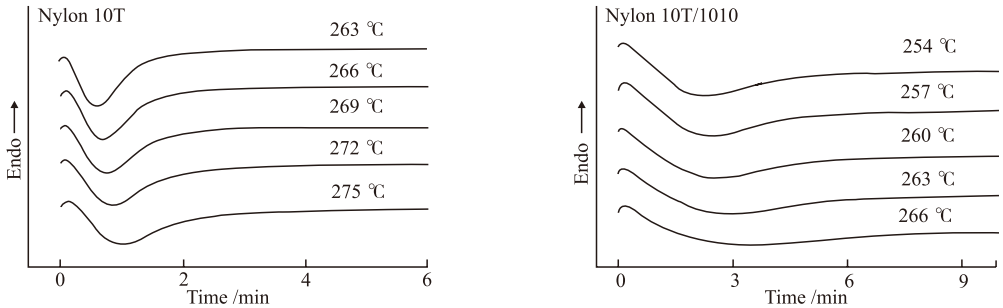

Fig.3 DSC curves of nylon 10T and nylon 10T/1010 isothermally crystallized at the specified temperatures

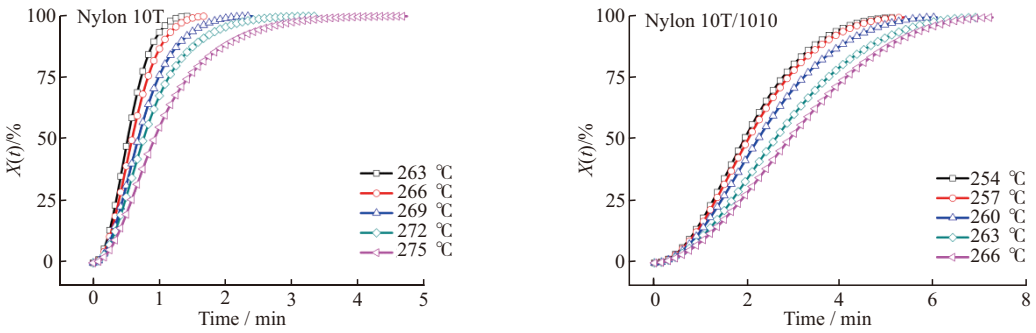

Fig.4 Relative crystallinity at different crystallization times during the process of isothermal crystallization for nylon 10T and nylon 10T/1010

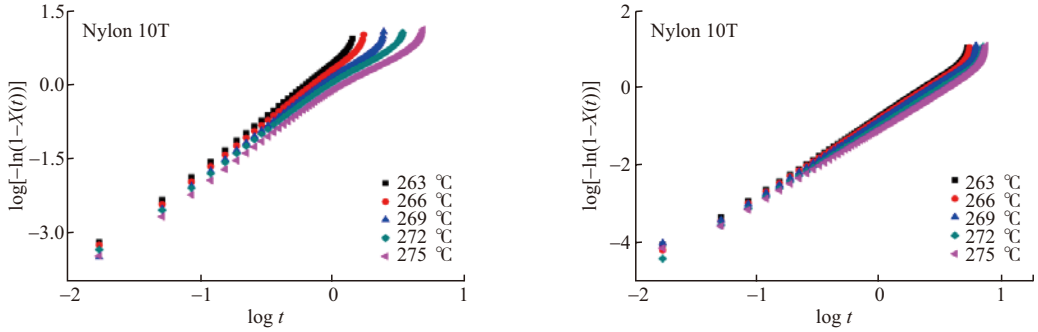

Fig.5 Plots of log[-ln(1-$X(t)$)] *versus* log t at the indicated temperature for the isothermal crystallization of nylon 10T and nylon 10T/1010

crystallization kinetics, the degree of crystalline conversion was measured as a function of time while keeping the temperature constant[21]. The relative crystallinity $X(t)$ at any crystallization time t is calculated as below[22]:

$$X(t)=\frac{X_c(t)}{X_c(t=\infty)}=\frac{\int_0^t \frac{dH_c(t)}{dt}dt}{\int_0^{t=\infty} \frac{dH_c(t)}{dt}dt} \quad (1)$$

where $dH_c(t)/dt$ is the rate of heat evolution. $X(t)$ is obtained from the area of the exothermic peak in the isothermal crystallization analysis using DSC, and is shown in Fig.4 with respect to time. It can be seen that the relative crystallinity decreased at a given crystallization time with an increase in crystallization temperature, suggesting that the crystallization rate decreased as temperature increased.

3.3 Analysis based on the Avrami theory

The crystallization process is highly temperature dependent, and consists of two distinct crystallization stages, primary and secondary[23]. The primary crystallization stage involves the outward clear growth of lamellar stacks, while the secondary crystallization stage is mainly due to the perfection of the internal spherulite crystallization and the spherulitic impingement in the later stage of the crystallization process[24,25]. In general, the Avrami theory can be employed to analyze the isothermal crystallization process of the nylon 10T and nylon 10T/1010 copolymers, based on the assumption that relative crystallinity $X(t)$ increases with the crystallization time t, as below[26]:

$$X(t)=1-\exp(-Kt^n) \quad (2)$$

To simplify the operation, Eq. (2) is usually written in a double logarithmic form as follows:

$$\log[-\ln(1-X(t))]=n\log t+\log K \quad (3)$$

where K is a crystallization rate constant involving both nucleation and crystal growth rate parameters, and n is a mechanism constant that depends on the form of nucleation and the growth dimension. Generally, the value of n should be an integer between 1 and 4 for different crystallization mechanisms. However, when other factors are involved in the process, such as competition of diffusion-controlled growth and/or the irregular boundary of the spherulites, then the Avrami exponent n will not be a simple integer any more[15]. Based on Eq.(3), the plots of log[-ln(1-$X(t)$)] *versus* log t were drawn, as shown in Fig.5. It can be seen that all the curves are divided into a primary crystallization stage and a secondary crystallization stage. The Avrami equation is generally assumed to be applicable only to the primary crystallization stage, thus the linear portion is approximately 30%-70% of the relative crystallinity for the isothermal crystallization process[27]. Accordingly, the Avrami exponent n and the

Table 1 Avrami kinetic parameters of the nylon 10T and the nylon 10T/1010 as function of crystallization temperature

Sample	T_c/℃	n	K/min^{-1}	$t_{1/2}$/min	$\tau_{1/2}$/min^{-1}	t_{max}/min
Nylon 10T	263	2.14	2.80	0.52	1.92	0.46
	266	2.08	2.10	0.59	1.71	0.51
	269	1.99	1.50	0.68	1.47	0.58
	272	1.84	1.15	0.76	1.32	0.60
	275	1.74	0.79	0.93	1.08	0.70
Nylon 10T/1010	254	2.00	0.19	1.92	0.52	1.63
	257	2.01	0.17	2.00	0.50	1.71
	260	1.95	0.15	2.22	0.45	1.85
	263	1.94	0.11	2.58	0.39	2.14
	266	1.97	0.09	2.88	0.35	2.42

crystallization rate K were obtained from the slope and intercept of the linear portion of Fig.5, respectively, and are presented in Table 1. Another important parameter in this regard is the crystallization half-time $t_{1/2}$, which is the time at which the extent of crystallization is 50%. The rate of crystallization $\tau_{1/2}$ is described as the reciprocal of $t_{1/2}$. The other related parameter, t_{max} is the time corresponding to the maximum crystallization rate, which can be calculated by Eq. (2)[28]. The values of $t_{1/2}$, $\tau_{1/2}$ and t_{max} are also presented in Table 1, and they were calculated using the equations below (Eqs.4-6):

$$t_{1/2} = \left(\frac{\ln 2}{K}\right)^{1/n} \tag{4}$$

$$\tau_{1/2} = \frac{1}{t_{1/2}} \tag{5}$$

$$t_{max} = \left(\frac{n-1}{nK}\right)^{1/n} \tag{6}$$

From the data in Table 1, it can be seen clearly that the Avrami exponent n decreases as the isothermal crystallization temperature increases. At the primary crystallization stage, the n values for nylon 10T and nylon 10T/1010 range from 1.74 to 2.14 and 1.94 to 2.01, respectively, which means that the addition of the sebacic acid comonomer does not noticeably influence the mechanism of the nucleation and the growth of the nylon 10T crystallites. These results also indicate that the nucleation and growth modes at the primary crystallization stage of the isothermal crystallization for the nylon 10T and nylon 10T/1010 samples may be a mixture of one-dimensional, needle-like growth and two-dimensional, circular growth, diffusion controlled growth with thermal nucleation. The dependency of $t_{1/2}$ on the crystallsization temperature is illustrated in Fig.6. Generally, $t_{1/2}$ is used to characterize the crystallization rate, and the longer the $t_{1/2}$, the slower the crystallization rate. At a certain crystallization temperature, the $t_{1/2}$ value of nylon 10T/1010 was higher than that of nylon 10T, *i e*, the crystallization rate of the former was slower than that of the latter.

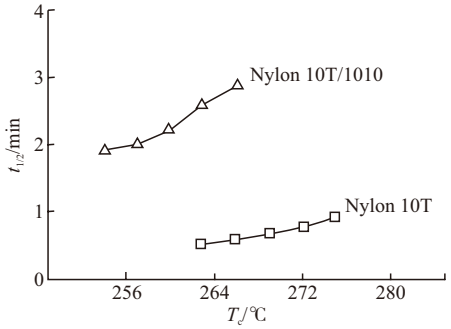

Fig.6 Crystallization half-time as a function of crystallization temperature for nylon 10T and nylon 10T/1010

3.4 Equilibrium melting point

For quantitative analysis of the crystallization behavior, especially the examination of the temperature dependence of the crystallization rate, it is essential to determine the equilibrium melting point as accurately as possible[29]. According to Hoffman-Weeks theory[30], the equilibrium melting point T_m^0 may be deduced by plotting the observed apparent melting temperature T_m with respect to the isothermal crystallization temperature T_c, which is obtained by extrapolation of the resulting straight line to intersect the line T_m=T_c[31], as follows:

$$T_m = \frac{T_c}{2\beta} + T_m^0\left(1 - \frac{1}{2\beta}\right) \tag{7}$$

where β denotes the growth of lamellar thickness during isothermal crystallization[32]. The plots of

T_m *versus* T_c are shown in Fig.7. The values of T_m^0 for nylon 10T and nylon 10T/1010 are found to be 316.18 and 322.33 ℃, respectively. In addition, the crystallization of polymers is generally influenced by the super-cooling degree ($\Delta T=T_m^0-T_c$), thus the plots of n versus ΔT or log K *versus* ΔT should be linear. The plots of n versus ΔT and log K *versus* ΔT for nylon 10T and nylon 10T/1010 are illustrated in Fig.8. It is evident that the values of n and log K for nylon 10T/1010 did not show a good linear relationship with respect to ΔT, which indicates that the addition of the sebacic acid comonomer significantly influenced the crystallization of nylon 10T.

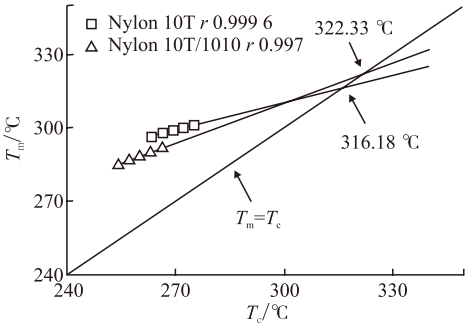

Fig.7 Melting temperatures as a function of crystallization temperatures for nylon 10T and nylon 10T/1010

3.5 Isothermal crystallization activation energy

Based on the assumption that the isothermal crystallization process is thermally activated, the approximate activation energy can be calculated by the following form of the Arrhenius equation[33]:

$$K^{1/n} = K_0 \exp(-\Delta E / RT_c) \tag{8}$$

Eq.(8) can be rewritten in a logarithmic form as:

$$\frac{1}{n}\ln K = \ln K_0 - \frac{\Delta E}{RT_c} \tag{9}$$

where K_0 and K values describe the pre-exponential factor and the crystallization rate constant, respectively. R is the universal gas constant. Then, by plotting $(1/n)$ ln K *versus* $1/T_c$, a straight line must be obtained with a slope equal to ΔE, as shown in Fig.9. ΔE is the sum of the activation energies for the nucleation and crystal growth processes in the isothermal crystallization process. The lower ΔE is, the faster the crystallization rate becomes[16]. Thus, ΔE value of nylon 10T/1010 was higher than that of nylon 10T, indicating that the crystallization ability of the nylon 10T/1010 was lower during the isothermal crystallization process. This is likely due to the addition of the sebacic acid comonomer which affects the symmetry and regularity of the polymer chains. This result is in accordance with that obtained from Avrami theory.

The Turnbull-Fisher equation, which is an important expression for spherulitic growth rate, can be expressed as follows[34]:

$$\ln G = \ln G_0 - \frac{\Delta E^*}{kT_c} - \frac{\Delta F^*}{kT_c} \tag{10}$$

where G is the spherulitic growth rate, G_0 is a pre-exponential factor, k is the Boltzmann constant, ΔE^* is the free energy of activation for transporting a chain segment from the super-cooled phase to the crystalline phase, and ΔF^* is the free energy of formation of a nucleus of critical size. At high temperature, the nucleation term, $\Delta F^*/kT_c$, is dominant. Therefore, as the crystallization temperature approaches the melting temperature, Eq. 10 can be written as follows[23]:

$$\ln G = \ln G_0 - \frac{\Delta F^*}{kT_c} \tag{11}$$

or

$$\ln G = \ln G_0 - \frac{\chi T_m^0}{T_c^2(T_m^0 - T_c)} \tag{12}$$

where χ is a parameter concerning the interfacial free energy and heat of fusion. According to Lin [35], the following equation can be obtained from Eqs. (2), (6) and (12):

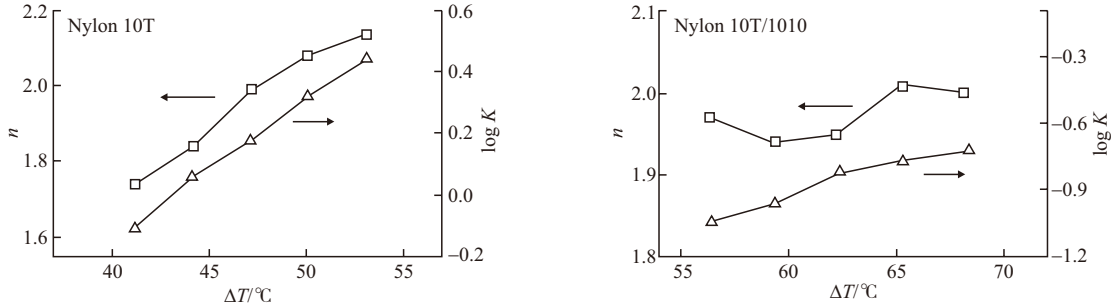

Fig.8 Plots of n *versus* ΔT and log K *versus* ΔT for nylon 10T and nylon 10T/1010

$$\log t_{\max} = \mathrm{B} - \frac{\mathrm{C}}{2.303 \cdot T_c^2 \cdot \Delta T} \tag{13}$$

where B and C are constants. Eq.(13) can be used to evaluate whether the primary stage of the isothermal crystallization of nylon 10T and nylon 10T/1010 could be described by the Avrami equation. In other words, if the plot of log t_{max} *versus* $1/(2.303T_c^2\Delta T)$ is a straight line, then it is very likely that nylon 10T or nylon 10T/1010 can be described as undergoing the primary stage of the isothermal crystallization. The plots for nylon 10T and nylon 10T/1010 show a good linear relationship, as shown in Fig.10.

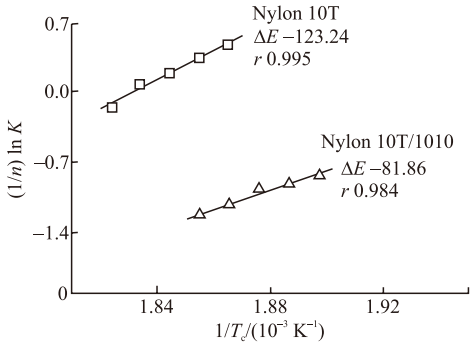

Fig.9 Plots of $1/n$ (ln K) *versus* $1/T_c$ for nylon 10*T* and nylon 10*T*/1010

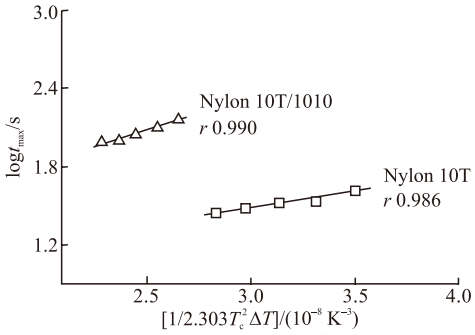

Fig.10 Plots of log t_{max} *versus* $1/(2.303T_c^2\Delta T)$ for nylon 10T and nylon 10T/1010

3.6 Lauritzen-Hoffman theory

In order to make the Turnbull-Fisher equation suitable for the isothermal crystallization process with a large degree of super-cooling, Lauritzen and Hoffman analyzed the spherulitic growth rate G and obtained the famous Lauritzen-Hoffman equation, as below[36,37]:

$$G = G_0 \exp\left(\frac{-U^*}{R\left(T_c - T_\infty\right)}\right) \exp\left(\frac{-K_g}{T_c \Delta T f}\right) \tag{14}$$

For convenience, Eq. (14) can be rearranged and written as follows:

$$\ln G + \frac{U^*}{R\left(T_c - T_\infty\right)} = \ln G_0 - \frac{K_g}{T_c \Delta T f} \tag{15}$$

where G is the growth rate of crystallization, defined as $G=1/(t_{1/2})$, which is obtained from Eq.(4)[38]. G_0 is a pre-exponential factor that includes all temperature independent terms, R is the universal gas constant and K_g is the nucleation parameter that reflects the regime behavior. U^* represents the diffusional activation energy for the transport of segments to the crystallizable site at the liquid-solid interface, taken as 6 280 J•mol^{-1}[22]. T_∞ is the hypothetical temperature where all motion associated with viscous flow ceases, which is usually assumed to be equal to (T_g-30) K. ΔT is the super-cooling degree, and f is a correction factor to account for the variation in the bulk enthalpy of fusion per unit volume with temperature, defined as $f=2T_c/(T_m^0+T_c)$. The plots of ln$G$+U*/[R(T_c-T_∞)] with respect to $1/(T_c\Delta Tf)$ should yield a straight line with a slope K_g and an intercept ln G_0, as shown in Fig.11. It can be seen that the K_g value of nylon 10T/1010 was higher than that of nylon 10T.

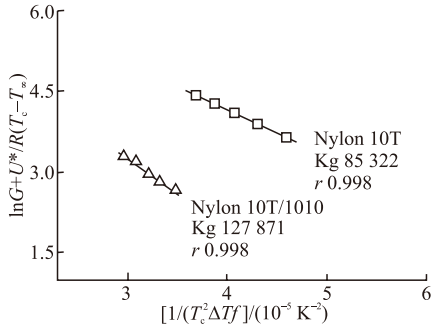

Fig.11 Plots of ln$G$+U*/[$R(T_c-T_\infty)$] *versus* $1/(T_c\Delta Tf)$ for nylon 10T and nylon 10T/1010

3.7 Crystal morphology

Polarization microscopic images of nylon 10T and nylon 10T/1010 are shown in Fig.12. It was found that the Maltese cross characteristic of spherulitic structures could not be observed in the images. From a comparison of the two photographs, it can be seen that nylon 10T contains relatively larger crystalline grains, whereas a denser granular texture of crystals is formed for nylon 10T/1010 with smaller crystalline grains. It is clear that the number of crystal nuclei is increased and the growth rate of crystalline grains is decreased by the addition of the sebacic acid comonomer. As the symmetry and regularity of the polymer chains are destroyed by the sebacic acid comonomer for nylon 10T/1010, its intracrystalline flaws are increased and crystal growth is restricted.

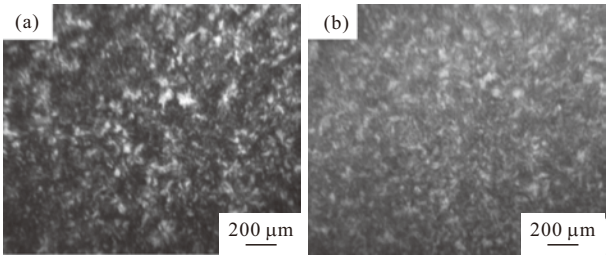

Fig.12 Crystal morphologies of samples by POM: (a) nylon 10T, observed at 269℃; (b) nylon 10T/1010, observed at 260℃

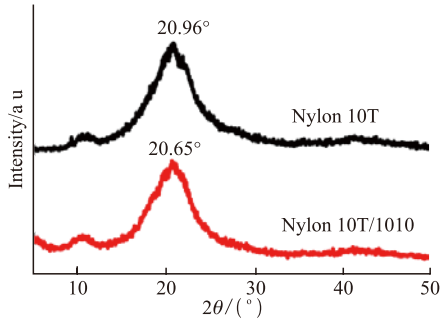

Fig.13 XRD patterns of nylon 10T and nylon 10T/1010

Table 2 XRD data of nylon 10T and nylon 10T/1010 by MDI Jade 5.0

Sample	2θ/(°)	Interplanar spacing/Å	Intensity /a u	Spherulitic size/Å
Nylon 10T	20.96	4.23	2 196	152
Nylon 10T/1010	20.65	4.30	1 995	131

The XRD patterns of nylon 10T and nylon 10T/1010 are presented in Fig.13. Compared to nylon 10T, the characteristic peaks of nylon 10T/1010 are almost unchanged. This indicates that the incorporation of sebacic acid comonomer into the nylon 10T did not change its crystalline form. All the XRD data are listed in Table 2. Compared with nylon 10T, it was observed that the size of crystalline grains of nylon 10T/1010 decreased, which is consistent with POM results.

4 Conclusions

A systematic investigation of the isothermal crystallization kinetics and morphology of nylon 10T and nylon 10T/1010 copolymers prepared by direct melt polymerization has been carried out. For the isothermal crystallization of nylon 10T and nylon 10T/1010, the crystallization peaks of the polymer shifted to the right and became flatter with increasing crystallization temperature. Avrami equation analysis reveals that the isothermal crystallization curves are divided into a primary crystallization stage and a secondary crystallization stage. At the primary crystallization stage, the n values for nylon 10T and nylon 10T/1010 ranged from 1.74 to 2.14 and 1.94 to 2.01, respectively, which meant that the nucleation and crystal growth modes are possibly a combination of one-dimensional, needle-like growth and two-dimensional, circular growth, diffusion controlled growth with thermal nucleation. The activation energies for isothermal crystallization of nylon 10T and nylon 10T/1010 have been determined by Arrhenius equation to be −123.24 and −81.86 kJ·mol^{-1}, respectively, which reveals that the crystallization ability of nylon 10T/1010 was lower. Combined with the results of the Turnbull-Fisher equation, the Avrami equation successfully describes the isothermal crystallization process of nylon 10T and nylon 10T/1010. POM and XRD observations showed that the addition of the sebacic acid comonomer did not affect the crystal form of nylon 10T, but significantly decreased the size and increased the number of spherulites.

References

[1] Chen J, Beake BD, Bell GA, *et al*. Investigation of the Nanomechanical Properties of Nylon 6 and Nylon 6/Clay Nanocomposites at Sub-Ambient Temperatures[J]. *Journal of Experimental Nanoscience*, 2016, 11(9): 695-706

[2] Wang WZ, Zhang YH. Environment-Friendly Synthesis of Long Chain Semiaromatic Polyamides[J]. *Express Polymer Letters*, 2009, 3(8): 470-476

[3] Wang WZ, Zhang YH. Synthesis of Semiaromatic Polyamides Based on Decanediamine[J]. *Chinese Journal of Polymer Science*, 2010, 28(4): 467-473

[4] Zhang CL, Wan L, Gu XP, *et al*. A Study on a Prepolymerization Process of Aromatic-Contained Polyamide Copolymers Pa(66-co-6T) via One-Step Polycondensation[J]. *Macromolecular Reaction Engineering*, 2015, 9(5): 512-521

[5] Rwei SP, Tseng YC, Chiu KC, *et al*. The Crystallization Kinetics of Nylon 6/6T and Nylon 66/6T Copolymers[J]. *Thermochimica Acta*, 2013, 555(5): 37-45

[6] Uddin AJ, Ohkoshi Y, Gotoh Y, *et al*. Influence of Moisture on the Viscoelastic Relaxations in Long Aliphatic Chain Contained Semiaromatic Polyamide, (PA9-T) Fiber[J]. *Journal of Polymer Science Part B-Polymer Physics*, 2003, 41(22): 2 878-2 891

[7] Uddin AJ, Gotoh Y, Ohkoshi Y, *et al*. Hydration in a New Semiaromatic Polyamide Observed by Humidity-Controlled Dynamic Viscoelastometry and X-ray Diffraction[J]. *Journal of Polymer Science Part B-Polymer Physics*, 2005, 43(13): 1 640-1 648

[8] Wang WZ, Wang XW, Li RX, *et al*. Environment-Friendly Synthesis of Long Chain Semiaromatic Polyamides with High Heat Resistance[J]. *Journal of Applied Polymer Science*, 2009, 114(4): 2 036-2 042

[9] Zhang CH, Huang XB, Zeng XB, *et al*. Fluidity Improvement of Semiaromatic Polyamides: Modification with Oligomers[J]. *Journal of Applied Polymer Science*, 2014, 131(7): 5 621-5 633

[10] Novitsky TF, Mathias LJ. One-Pot Synthesis of Polyamide 12,T-polyamide-6 Block Copolymers[J]. *Journal of Polymer Science Part A-Polymer Chemistry*, 2011, 49(10): 2 271-2 280

[11] Novitsky TF, Mathias LJ, Osborn S, *et al*. Synthesis and Thermal Behavior of Polyamide 12,T Random and Block Copolymers[J]. *Macromolecular Symposia*, 2012, 313-314(1): 90-99

[12] Novitsky TF, Lange CA, Mathias LJ, *et al*. Eutectic Melting Behavior of Polyamide 10,T-co-6,T and 12,T-co-6,T Copolyterephthalamides[J]. *Polymer*, 2010, 51(11): 2 417-2 425

[13] Battegazzore D. Bulk *Vs* Surface Flame Retardancy of Fully Bio-Based Polyamide 10,10[J]. *RSC Advances*, 2015, 5(49): 39 424-39 432

[14] Dong JX, Qu JH, Feng XY, *et al*. Development Status and Prospects of World Bio-Based Polyamides[J]. *China Synthetic Fiber Industry*, 2015, 38(5): 51-56 (in Chinese)

[15] Zhang XK, Xie TX, Yang GS. Isothermal Crystallization and Melting Behaviors of Nylon 11/Nylon 66 Alloys by *in Situ* Polymerization[J]. *Polymer*, 2006, 47(6): 2 116-2 126

[16] Ferreira CI, Castel CD, Oviedo MAS, *et al*. Isothermal and Non-Isothermal Crystallization Kinetics of Polypropylene/Exfoliated Graphite Nanocomposites[J]. *Thermochimica Acta*, 2013, 553(3): 40-48

[17] Neugebauer F, Ploshikhin V, Ambrosy J, *et al*. Isothermal and Non-Isothermal Crystallization Kinetics of Polyamide 12 Used in Laser Sintering[J]. *Journal of Thermal Analysis and Calorimetry*, 2016, 124(2): 925-933

[18] Gradys A, Sajkiewicz P, Zhuravlev E, *et al*. Kinetics of Isothermal and Non-Isothermal Crystallization of Poly(Vinylidene Fluoride) by Fast Scanning Calorimetry[J]. *Polymer*, 2016, 82: 40-48

[19] Zhang YS, Wang BB, Hu GS. Isothermal Crystallization Kinetics and Melting Behavior of Polyamide 11/Silica Nanocomposites Prepared by *in Situ* Melt Polymerization[J]. *Journal of Applied Polymer Science*, 2012, 123(1): 273-279

[20] Shashidhara GM, Pradeepa KG. Isothermal Crystallization of Polyamide 6/Liquid Natural Rubber Blends at High under Cooling[J]. *Thermochimica Acta*, 2014, 578(4): 1-9

[21] Liu HX, Huang YY, Yuan L, *et al*. Isothermal Crystallization Kinetics of Modified Bamboo Cellulose/PCL Composites[J]. *Carbohydrate Polymers*, 2010, 79(3): 513-519

[22] Cai J, Liu M, Wang L, *et al*. Isothermal Crystallization Kinetics of Thermoplastic Starch/Poly(Lactic Acid) Composites[J]. *Carbohydrate Polymers*, 2011, 86(2): 941-947

[23] Liu SY, Yu YN, Yi C, *et al*. Isothermal and Nonisothermal Crystallization Kinetics of Nylon-11[J]. *Journal of Applied Polymer Science*, 1998, 70(12): 2 371-2 380

[24] Ge CH, Ding P, Shi LY, *et al*. Isothermal Crystallization Kinetics and Melting Behavior of Poly(Ethylene Terephthalate)/Barite Nanocomposites[J]. *Journal of Polymer Science Part B-Polymer Physics*, 2009, 47(7): 655-668

[25] Run MT, Song HZ, Wang SJ, *et al*. Crystal Morphology, Melting Behaviors and Isothermal Crystallization Kinetics of SCF/PTT Composites[J]. *Polymer Composites*, 2009, 30(1): 87-94

[26] He H, Gu LX, Ozaki Y. Non-Isothermal Crystallization and Thermal Transitions of a Biodegradable, Partially Hydrolyzed Poly (Vinyl Alcohol)[J]. *Polymer*, 2006, 47(11): 3 935-3 945

[27] Liao RG, Yang B, Yu W, *et al*. Isothermal Cold Crystallization Kinetics of Polylactide/Nucleating Agents[J]. *Journal of Applied Polymer Science*, 2007, 104(1): 310-317

[28] Liu MY, Zhao QX, Wang YD, *et al*. Melting Behaviors, Isothermal and Non-Isothermal Crystallization Kinetics of Nylon 1212[J]. *Polymer*, 2003, 44(8): 2 537-2 545

[29] Zou P, Tang SW, Fu ZZ, *et al*. Isothermal and Non-Isothermal Crystallization Kinetics of Modified Rape Straw Flour/High-Density Polyethylene Composites[J]. *International Journal of Thermal Sciences*, 2009, 48(4): 837-846

[30] Hoffman JD, Miller RL. Kinetic of Crystallization From the Melt and Chain Folding in Polyethylene Fractions Revisited: Theory and Experiment[J]. *Polymer*, 1997, 38(13): 3 151-3 212

[31] Cai J, Liu M, Wang L, *et al*. Isothermal Crystallization Kinetics of Thermoplastic Starch/Poly(Lactic Acid) Composites[J]. *Carbohydrate Polymers*, 2011, 86(2): 941-947

[32] Kalkar AK, Deshpe VD, Kulkarni MJ. Isothermal Crystallization Kinetics of Poly(Phenylene sulfide)/TLCP Composites.[J]. *Polymer Engineering and Science*, 2009, 13(s 1-4): 651-654

[33] Tjong SC, Chen SX, Li RKY. Crystallization Kinetics of Compatibilized Blends of a Liquid Crystalline Polymer with Polypropylene[J]. *Journal of Applied Polymer Science*, 1997, 64(4): 707-715

[34] Biber E, Gündüz G, Mavis B, *et al*. Compatibility Analysis of Nylon 6 and Poly(Ethylene-N-Butyl Acrylate-Maleic Anhydride) Elastomer Blends Using Isothermal Crystallization Kinetics[J]. *Materials Chemistry and Physics*, 2010, 122(1): 93-101

[35] Lin CC. The Rate of Crystallization of Poly(Ethylene Terephthalate) by Differential Scanning Calorimetry[J]. *Polymer Engineering and Science*, 1983, 23(3): 113-116

[36] Zhu G, Li CC, Li ZY. The Effects of Alkali Dehydroabietate on the Crystallization Process of Polypropylene[J]. *European Polymer Journal*, 2001, 37(5): 1 007-1 013

[37] Neugebauer F, Ploshikhin V, Ambrosy J, *et al*. Isothermal and Non-Isothermal Crystallization Kinetics of Polyamide 12 Used in Laser Sintering[J]. *Journal of Thermal Analysis and Calorimetry*, 2016, 124(2): 925-933

[38] Liu TX, Mo ZS, Wang SE, *et al*. Isothermal Melt and Cold Crystallization Kinetics of Poly(Aryl Ether Ether Ketone Ketone) (PEEKK)[J]. *European Polymer Journal*, 1997, 33(9): 1 405-1 414